Uncertainty analysis in quantitative integration of inverted 3D seismic data for static reservoir modeling

Mohammad Emami Niri* and David Lumley, Centre for Petroleum Geoscience and CO2 Sequestration, University of Western Australia

Abstract

It is common practice to quantitatively integrate 3D seismic data in reservoir property modeling. Seismic data, due to its high areal coverage, can improve interpolation of the reservoir properties beyond the wells. However, it is important to clarify the limits of quantitative use of 3D seismic data in reservoir characterization and modeling. Our analyses show that quantitative integration of inverted 3D seismic data in static reservoir modeling carries a range of uncertainties and should be cautiously applied in order to minimize the risk of misinterpretation. In this study, we investigate the uncertainties and limitations in quantitative incorporation of deterministic seismic inversion results in reservoir litho-facies modeling. These uncertainties are due to the limited seismic resolution compared to the scale of the geological heterogeneities; and the non-unique elastic properties of different facies types. To do this we employ a seismic constraining method ("Probability of facies distribution given by P-wave impedance") on a geostatistical simulation technique to construct seismically-constrained litho-facies models. We then compare the results with the true reference litho-facies model to identify uncertainties caused by limited seismic resolution, errors in the predicted elastic properties and non-unique rock properties.

Introduction

Subsurface heterogeneity influences resource/reserve assessment and reservoir production. Due to the limited spatial distribution of well data, it is not an easy task to estimate an accurate distribution of reservoir and rock properties between wells. However, we can take advantage of the high spatial coverage of seismic data, and use it to constrain the reservoir facies and petrophysical property interpolation process. This can be performed for example by using geostatistical simulation techniques (Doyen, 2007).

Seismic inversion is commonly used in the estimation of the Earth's elastic properties (e.g. impedances, velocities) from seismic data. The scope of seismic reservoir characterization, however, goes beyond inverting for the elastic parameters and attempts to obtain the reservoir properties such as lithofacies, porosity, pressure and saturation from the seismic-related data (Dupin et al, 2011). To do this, a conventional approach would be to use a deterministic relationship between seismic attributes like impedance and reservoir properties such as porosity. Another common approach is the incorporation of seismic attributes (e.g. impedance or amplitude) as secondary information in the geostatistical simulation of the reservoir properties. There are some examples of the application of these two approaches over the past decades (Angeleri and Carpi 1982; Dubrule 2003; Nivlet et al. 2005; Doyen 2007). The technical bottlenecks associated with these applications, such as the difference in scale and support at which the measurement was made and the low frequency content of the seismic data, can lead to incorrect results (Francis 2010).

This paper gives an overview of how the synthetic datasets for this study were constructed, followed by a discussion on the implementation of a seismically-constrained method to the static reservoir modeling process. Then we investigate the uncertainties in the integration of 3D seismic data in the lithofacies modeling by addressing the limited seismic vertical resolution and overlapping elastic properties of different facies types.

Test model

In this study we generate synthetic dataset (for simplicity, two lithology types and one elastic property) to address the uncertainties associated with the incorporation of inverted 3D seismic data in reservoir litho-facies modeling. First, we synthesize a base reservoir lithology model, consisting of 20% sand and 80% shale. We keep the NTG small to identify the uncertainties in prediction of the areas with low net sand thickness. The model covers an area of 6 km^2 and the reservoir gross thickness is 100 m. Upper and lower bounding pure shales are also 100 m thick. This 3D model contains 212 x 184 x 140 grid blocks with dimensions of 12.5x12.5x1 m^3. The sand and shale distributions within the reservoir interval are drawn using the SIS (Sequential Indicator Simulation) technique with exponential variogram parameters of 20 m vertical and 1000 m isotropic horizontal range for both sand and shale. The thickness of the sand bodies is ranging from below seismic resolution to above seismic resolution. The generated facies model (Figure 1) is assumed to be the

true reference litho-facies model for this synthetic case study. Seven well-trajectories are then constructed at randomly defined positions within the reservoir 3D framework, and the blocked litho-logs are obtained by identifying the grid blocks that intersect the well trajectories.

For the same base litho-facies model, we generate several P-impedance volumes using the SGS (Sequential Gaussian Simulation) technique with exponential variogram ranges of 10 m vertically and 1000 m in major and minor directions. Different impedance volumes are generated to have various degrees of overlapping P-impedance properties for sand and shale. We keep the mean of the distributions for all P-impedance models constant, 6500 g/cm^3.m/s for sand and 8500 g/cm^3.m/s for shale. But we change the standard deviation of the

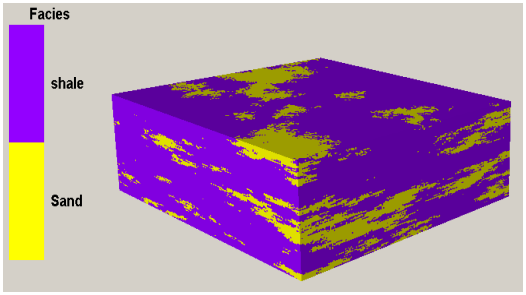

distributions for each separate P-impedance volume.

Figure 1: The base litho-facies model.

In addition, to simulate the limited frequency range of the deterministic inversion results, a moving average smoothing filter is applied to the impedance volumes. It replaces the data in each cell of the 3D volume with the average of the data in neighboring cells. This process is equivalent to a high-cut filtering of the 3D impedance volume. An example of the P-impedance histograms and high resolution 3D impedance volume with the standard deviation of 500 g/cm^3.m/s are shown in Figures 2a and 2b, and the effect of the applying a high-cut filter on the impedance model and the histograms can be observed in Figures 3a and 3b.

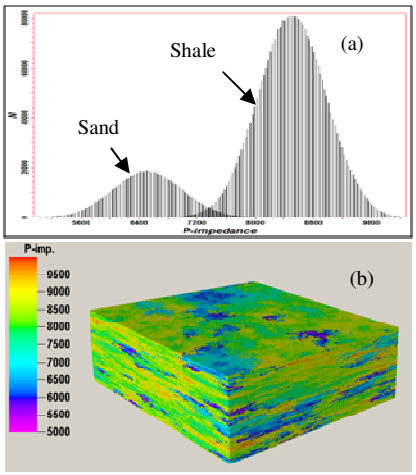

Figure 2: (a) The histograms of P-impedance distribution for sand and shale, (b) the high resolution P-impedance volume.

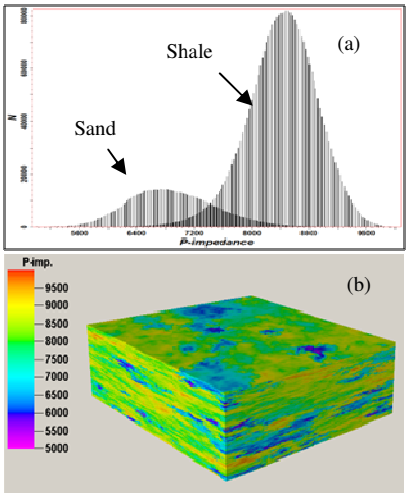

Figure 3: (a) The histograms of P-impedance distribution for sand and shale after high-cut filter, (b) the high-cut filtered P-impedance volume.

Integration of inverted 3D seismic data in litho-facies modeling

Emami Niri and Lumley (2013) studied five different constraining methods on a geostatistical simulation technique to construct seismically-constrained litho-facies models for two different case studies. They compared the results to determine which method produces the best match to the true reference model. The results of that study indicate that constraining method known as "probability of facies distribution given by P-wave impedance" gives the least misfit error of the five tested methods, even in the presence of realistic noise in the datasets. In addition, variogram parameter analysis suggests that, when the quality of seismic data is reliable, short variogram ranges can be used to accurately model the internal reservoir heterogeneity.

In this study we focus on the seismic constraining method "probability of facies distribution given by P-wave impedance" to construct the litho-facies models. First, a cross-plot analysis between facies indicators and P-wave impedance values at well locations is performed to determine the most suitable link between seismic and geological properties. This analysis produces a probability curve that can be used for the calibration and guiding of seismic attributes versus litho-facies indicators. Next, facies organization inside the reservoir is obtained by constraining the stochastic modeling process based on the results this analysis (Emami Niri and Lumley, 2013).

It is worthy to note that this probability function is dependent on the histogram of P-impedance distribution. For instance in Figure 4 the derived probability curves (blue curve) for high resolution and high-cut filtered P-impedance histograms (Figures 2a and 3a) are shown.

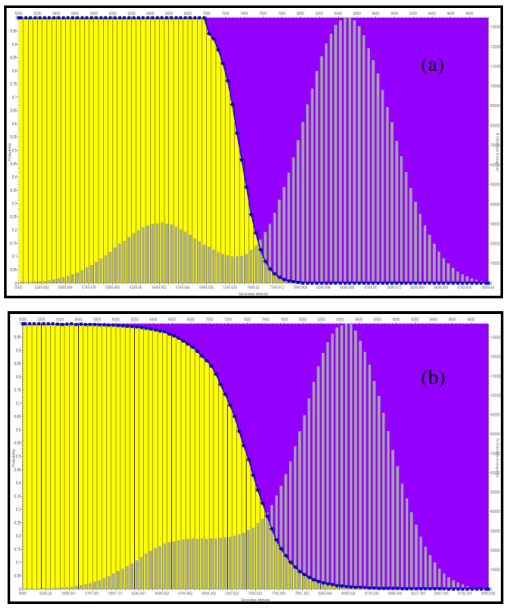

Figure 4: Probability of facies distribution (blue curve) derived from (a) the high resolution distribution of P-impedance, and (b) high-cut filtered distribution of P-impedance.

Uncertainty Analysis workflow

In this section, the workflow used for the uncertainty analysis is described. We first generate the net sand map of the base litho-facies model (Figure 5). It represents the actual net sand thickness of the reservoir interval. Second, we generate three impedance volumes for the same base litho-facies model, to have various degrees of overlapping P-impedance properties. This is done by keeping the means of the distributions for all three P-impedance volumes constant; 6500 g/cm^3.m/s for sand and 8500 g/cm^3.m/s for shale, and changing the standard deviation of the distributions from 0 in the first model to 500 and 1000 g/cm^3.m/s for the second and third models respectively (Figures 6 a-c).

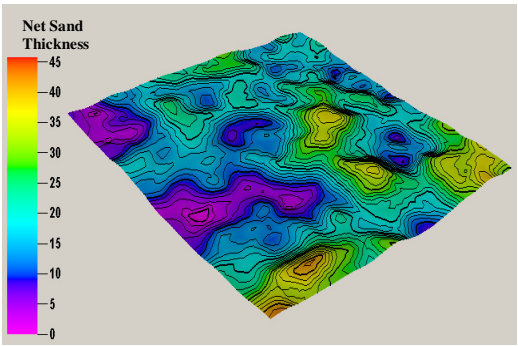

Figure 5: Net sand map in reference litho-facies model.

We then separately use each of the three P-impedance volumes to build seismically-constrained litho-facies models. This is achieved by deriving the probability curves at well locations for each case based on the method discussed in the previous section. The seismic constraining method is then applied to quantitatively integrate seismic data in the geostatistical litho-facies modeling process. Next, we generate the corresponding net sand maps from the constructed litho-facies models (Figures 6 d-f). Cross-plots of the actual net sand map versus predicted net sand maps derived from each case of the litho-facies simulation give an estimate of the uncertainty and biased errors in the prediction of the net sand in the reservoir interval (Figures 6 g-i).

Discussion

In this section, we highlight how the factors like various degrees of overlapping elastic properties and limited seismic resolution (which results in errors in estimating the elastic properties and increases the property overlap) affects the quantitative integration of the elastic properties in the litho-facies modeling. In Figure 6a we can see the standard deviation of P-impedance distribution is zero, meaning there is not any overlap between the P-impedance values of different lithology types. The corresponding crossplot analysis (Figure 6g) illustrates small uncertainty in the estimation of the net sand, with small underestimation in the areas of high net sand thickness. In Figures 6b and 6c, the overlap of the elastic properties of sand and shale increases and as a result, the uncertainty in the prediction of the net sand thickness increases. The respective cross plots in Figures 6h and 6i show that with increase in the overlap of elastic properties of sand and shale, the areas with low net sand thickness are overestimated and the areas of high net sand thickness are underestimated. An interesting point is that the corresponding errors in the net sand prediction are biased, and this bias varies with the degree of the non-unique overlap in elastic properties.

In another stage of this study we investigate the effects of the limited seismic resolution on the net sand prediction process. To do this, we applied a high-cut filter to a high resolution P-impedance volume to mimic the effect of the low frequency content of the deterministic seismic inversion. It is obvious that as the thickness of the sandy areas become smaller than the vertical seismic resolution limit, errors in the estimation of the elastic rock properties increase. This produces a significant increase to the overlapping area of the elastic properties (Figures 7a and 7b). The corresponding cross-plots of the actual versus estimated net sand (Figure 7c and 7d) indicate that the uncertainty in net sand prediction increases with a decrease in seismic resolution. In particular, we observe considerable over-prediction in the areas with low net sand.

Conclusions

Seismic data plays a significant role not only in defining the reservoir architecture, but also in constraining the

reservoir's discrete and continuous property models. In this paper, we address two fundamental uncertainties in quantitative integration of deterministic seismic inversion products in reservoir property modeling: limited seismic resolution and non-unique overlap of elastic properties for different lithologies. It is expected that with increasing overlap of the elastic properties of different lithology types, the uncertainty in the prediction of the net sand thickness increases. We show that this results in overestimation in areas with low net sand thickness, and underestimation in areas of high net sand thickness. Also, we show that when the overlap among elastic properties of different lithofacies types does not exist, a small amount of underestimation occurs in areas of high net sand thickness. This trend is reversed as the overlapping area increases. So, we conclude that the errors in the net sand prediction are biased, and the bias increases with the degree of non-unique overlap in elastic properties.

In addition, we see that as the thickness of the sand becomes smaller than seismic vertical resolution, errors in the estimation of the elastic rock properties increase, and this affects the degree of overlap in elastic properties of different litho-facies types. As a result, we observe considerable overestimation of sand in the areas of the low net sand thickness.

Acknowledgments

The authors would like to thank the UWA:RM industry research consortium sponsors, and the ASEG (Australian Society of Exploration Geophysicists) Research Fund, for providing partial research funding for this work. We also acknowledge Schlumberger for use of the Petrel software package.

References

Angeleri G.P., and Carpi R., 1982, Porosity prediction from seismic data. Geophys. Prospect, 30, No.5, 580-670.

Doyen, P.M., 2007, Seismic Reservoir Characterization, an Earth Modelling Perspective, European Association of Geoscientists and Engineers press.

Dubrule, O., 2003, Geostatistics for seismic data integration in earth models, SEG/EAGE distinguished instructor short course no. 6.

Dupin, M., Baroni, G., Da Veiga, S., 2011, Preselection of reservoir models from a geostatistics-based petrophysical seismic inversion. SPE Reservoir Evaluation and Engineering,Vol.14, No.5, 612-620.

Emami Niri M., and Lumley D., 2013. Initializing dynamic reservoir models for history matching using preproduction 3D seismic data. 6th IPTC, Beijing-China, March 26-28, IPTC 16650.

Francis A., 2010. Limitations of deterministic seismic inversion data as input for reservoir model conditioning, SEG annual meeting, Denver.

Nivlet P., Lucet N., Albouy E., Lerat O., Doligez B., Roggero F., Lefeuvre F., Piazza J.L, Brechet E., Duplantier O., Vittori J., Berthet P., 2005. Facies analysis from prestack inversion results in a deep offshore turbidite reservoir, SEG annual meeting, Houston, Texas.

Sams M.S. and Saussus, 2010. Uncertainties in the quantitative interpretation of lithology probability volumes. LeadingEdge,No.29,vol.5,576-583.

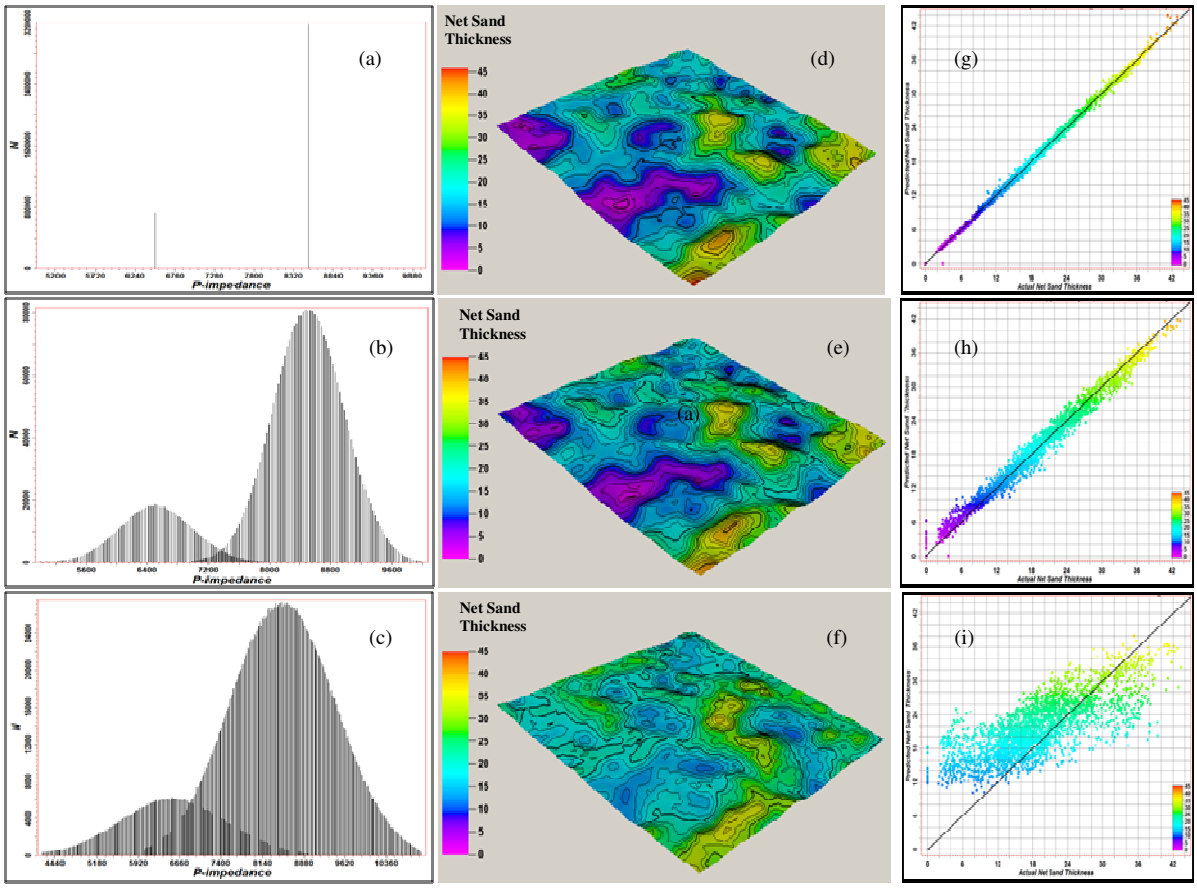

Figure 6: (a-c) The histograms of P-impedance distributions for sand and shale, (d-f) the net sand maps derived from the simulated litho-facies models, (g-i) the corresponding cross-plot of the actual versus predicted net sand.

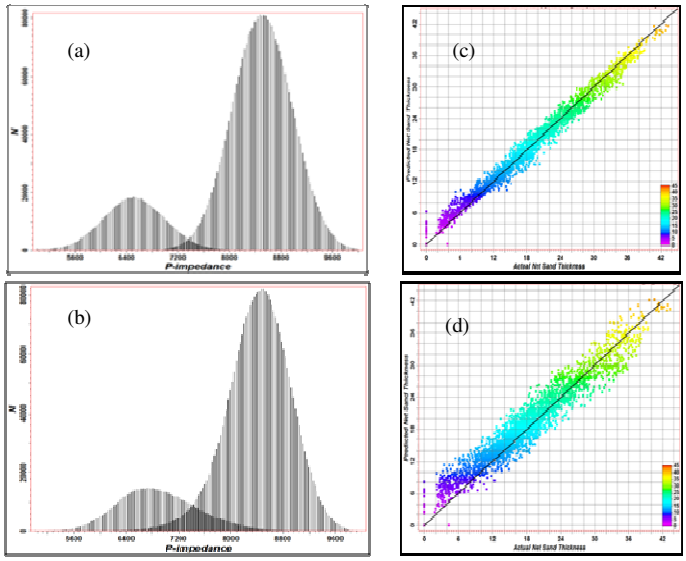

Figure 7: (a-b) The histograms of the P-impedance distribution for a high resolution volume and a high-cut filtered volume, (c-d) the respective actual versus estimated net sand cross-plots.